Available online at www.sciencedirect.com
ScienceDirect
Talanta 74 (2008) 518–525
Talanta
www.elsevier.com/locate/talanta

Double interdigitated array microelectrode-based impedance biosensor for detection of viable *Escherichia coli* O157:H7 in growth medium

Madhukar Varshney [a], Yanbin Li [a,b,*]

[a] *Department of Biological and Agricultural Engineering, University of Arkansas, Fayetteville, AR 72701, United States*
[b] *Center of Excellence for Poultry Science, University of Arkansas, Fayetteville, AR 72701, United States*

Received 12 March 2007; received in revised form 13 June 2007; accepted 13 June 2007
Available online 30 June 2007

Abstract

Double interdigitated array microelectrodes (IAM)-based flow cell was developed for an impedance biosensor to detect viable *Escherichia coli* O157:H7 cells after enrichment in a growth medium. This study was aimed at the design of a simple flow cell with embedded IAM which does not require complex microfabrication techniques and can be used repeatedly with a simple assembly/disassembly step. The flow cell was also unique in having two IAM chips on both top and bottom surfaces of the flow cell, which enhances the sensitivity of the impedance measurement. *E. coli* O157:H7 cells were grown in a low conductivity yeast–peptone–lactose–TMAO (YPLT) medium outside the flow cell. After bacterial growth, impedance was measured inside the flow cell. Equivalent circuit analysis indicated that the impedance change caused by bacterial growth was due to double layer capacitance and bulk medium resistance. Both parameters were a function of ionic concentration in the medium, which increased during bacterial growth due to the conversion of weakly charged substances present in the medium into highly charged ions. The impedance biosensor successfully detected *E. coli* O157:H7 in a range from 8.0 to 8.2×10^8 CFU mL^{-1} after an enrichment growth of 14.7 and 0.8 h, respectively. A logarithmic linear relationship between detection time (T_D) in h and initial cell concentration (N_0) in CFU mL^{-1} was $T_D = -1.73 \log N_0 + 14.62$, with $R^2 = 0.93$. Double IAM-based flow cell was more sensitive than single IAM-based flow cell in the detection of *E. coli* O157:H7 with 37–61% more impedance change for the frequency from 10 Hz to 1 MHz. The double IAM-based flow cell can be used to design a simple impedance biosensor for the sensitive detection of bacterial growth and their metabolites.

Keywords: Impedance detection; Impedance microbiology; *E. coli* O157:H7; Interdigitated array microelectrodes; Flow cell

1. Introduction

Impedance microbiology is applied in a variety of fields ranging from detection and monitoring of microorganisms, detection of antibiotics, analysis of food preservatives, food hygiene, and clinical and pharmaceutical microbiology to environmental sampling [1–6]. This indirect approach to quantitative microbiology quantifies microorganisms by measuring the change in the electrical conductivity of the medium during growth of microorganism [2]. It was first introduced by Stewart [7], however, this technique received the attention to merit only in mid seventies during last century. Growth of microorganisms increases the conductivity of the medium by converting uncharged or weakly charged substances present in the growth medium, such as yeast, peptone, and sugar into highly charged substances such as amino acids, aldehydes, ketones, acids, and other metabolic products [5]. Change in the conductivity of the solution during bacterial growth is recorded by impedance and conductance techniques. Detection time is inversely proportional to the initial numbers of cells present in the medium before growth. Therefore, a high number of cells result in a low detection time and vice versa. Edmiston [8] reported a detection time ranging from 1 to 7 h for the detection of a range of initial bacterial concentrations from 10^7 to 10^1 CFU mL^{-1}. Impedance measurement is commonly preferred over conductance measurement as it accounts for double layer capacitance and dielectric capacitance of the system in addition to the resistance (inverse of conductance) of the solution, while conductance measurement accounts for conductance of the solution only. It has been estimated that a minimum of 10^3 to 10^7 CFU mL^{-1} of bacterial cells are required to produce a detectable change in the impedance signal [9].

* Corresponding author at: Department of Biological and Agricultural Engineering, University of Arkansas, 230 Engineering Hall, Fayetteville, AR 72701, United States. Tel.: +1 479 575 2424; fax: +1 479 575 7139.
E-mail address: yanbinli@uark.edu (Y. Li).

0039-9140/$ – see front matter © 2007 Elsevier B.V. All rights reserved.
doi:10.1016/j.talanta.2007.06.027

Traditionally, thin metal rods or wires immersed in a medium were used as electrodes in the impedance measurement techniques [10–12]. In an attempt to improve sensitivities, add functionalities, and lower the detection limits of impedance techniques, several shapes of electrodes have been developed in last few decades. Of these, microelectrodes fabricated using lithographic techniques have been of great interest because they typically have higher sensitivities than macroelectrodes. The macroelectrodes have a semi-infinite linear diffusion profile resulting in a greater depletion of reactants in contrast to the microelectrodes which has a spherical diffusion profile favoring greater rate of reactant supply to the electrodes [13]. Among microelectrodes, IAM presents promising advantages in terms of low ohmic drop, fast establishment of steady state, rapid kinetics of reaction, and increased signal-to-noise ratio [14,15]. IAM are successfully employed for impedance measurement of bacterial cells during enrichment growth (impedance microbiology) [6,16–19], by capturing bacterial cells to the antibodies immobilized on the surface of electrodes (faradic impedance method) [20–24], or by using dielectrophoresis (DEP) for the capture of cells on the surface of electrodes (dielectrophoretic impedance) [25–29]. To enhance the capability of IAM in impedance sensing, microfluidic flow cells can be added to the IAM to achieve a fully integrated microchip for a broad range of applications including dielectrophoresis and impedance detection [30,31]. The advantages of microfluidic flow cells in combination with embedded IAM are: high detection sensitivity, small volume handling, low contamination during bacterial growth, ability to concentrate cells, and rapid detection of small number of cells. As the surface to volume ratio increases in the microfluidic flow cells with embedded IAM, the distance that conductive ions must diffuse to reach the sensor surface also decreases, thus resulting in rapid reaction kinetics [32]. Current impedance sensing techniques either employ an open IAM chip [16,17,20–24] or are based on the complex multi-step design of a flow cell with an embedded IAM [18,19,29–31], which have limited applications due to clogging and insufficient cleaning.

Selective medium is commonly used to give specificity to impedance detection system for the target bacteria. Yang et al. [16] used IAM-based impedance biosensor for rapid detection of viable *Salmonella* Typhimurium in a selective medium. selenite cystein (SC) broth supplemented with trimethylamine oxide (TMAO·HCl) and mannitol (SC/T/M) was used for the selective growth of *S*. Typhimurium. During the growth of three non-target bacteria (*Listeria monocytogenes*, *Escherichia coli* O157:H7, and *Pseudomonas aeruginosa*) in SC/T/M medium for 16 h, no significant change in the impedance response of the system was observed. The IAM-based biosensor was successfully used to detect a range of *S*. Typhimurium from 4.8 to 5.4×10^5 CFU mL^{-1} after an enrichment growth of 9.3 and 2.2 h, respectively. Non-selective medium can also be used for the impedance detection of bacterial cell growth. In this case, target bacteria from the sample can be separated and concentrated by immunoseparation with conjugated immunomagnetic microbeads. Yang and Li [17] demonstrated the use of general medium—brain heart infusion (BHI) broth, for the detection of *S*. Typhimurium using impedance technique. Anti-*Salmonella* antibodies coated magnetic microbeads were used to separate and concentrate *S*. Typhimurium from the samples followed by the growth of bacterial cells in BHI broth. The impedance measurement was most sensitive at 10 Hz and the IAM-based biosensor was able to detect initial concentrations of 10^1 and 10^6 CFU mL^{-1} of *S*. Typhimurium in a growth time of 8 and 1.5 h, respectively. Gomez-Sjöberg et al. [6] combined immunomagnetic separation and dielectrophoresis with impedance microbiology to design an on-site incubation microfluidic biochip with IAM to detect *Listeria* in a non-selective medium. IAM were used to concentrate bacterial cells by a factor of 10^4 to 10^5 in a detection chamber of volume 400 pL followed by an enrichment growth in a non-selective growth medium (Luria Bertani broth). The detection time for 8.4×10^4 CFU mL^{-1} of *L. monocytogenes* was less than 2 h.

In this study, we designed and tested a simple double IAM-based flow cell for an impedance biosensor to detect viable *E. coli* O157:H7 cells from the samples after an enrichment growth in a low conductivity growth medium. This flow cell with embedded IAM could be easily assembled without the need of complicated microfabrication techniques. The flow cell could also be easily disassembled to clean the electrode for repeated use. The flow cell was also unique by using double IAM on its top and bottom surfaces to enhance the sensitivity in the detection of *E. coli* O157:H7. The impedance change was due to the growth of *E. coli* O157:H7 cells that was analyzed as a function of frequency. An equivalent circuit was designed to curve fit experimental results and to determine parameters of the electrical circuit responsible for impedance change caused by the growth of *E. coli* O157:H7 cells.

2. Experimental

2.1. Bacterial culture and chemicals

Frozen stock of *E. coli* O157:H7 (ATCC 43888) was maintained in brain heart infusion (with 12% glycerol) broth (Remel Inc., Lenexa, KS) at −70 °C. Culture was harvested in brain heart infusion broth maintained at 37 °C for 18–22 h. For enumeration, pure cultures were serially diluted in 0.01 M, pH 7.4 phosphate-buffered saline and surface plated on sorbitol MacConkey agar (Remel Inc., Lenexa, KS), which was incubated at 37 °C for 20–22 h. Yeast extract (BD Inc., Franklin Lakes, NJ), peptone (BD Inc., Franklin Lakes, NJ), lactose (Sigma–Aldrich, St. Louis, MI), and trimethylamine oxide (TMAO, Sigma–Aldrich, St. Louis, MI) were used for the low conductivity growth medium for the enrichment growth of bacterial cells.

2.2. Enrichment growth medium and bacterial growth

Specially designed low conductivity yeast–peptone–lactose–TMAO (YPLT) medium was prepared by mixing yeast extract (10 g/L), peptone (5 g/L), lactose (3.3 g/L), and TMAO (5.0 g/L) in deionized water. The medium was autoclaved at 121 °C for 15 min. Salts such as sodium chloride and disodium phosphate were not added in order to minimize the conductivity of the medium. Growth medium was optimized for the growth of

E. coli O157:H7 cells. Lactose was preferred over the use of glucose, as *E. coli* O157:H7 cells cannot metabolize glucose. TMAO was used for the optimum growth of *E. coli* O157:H7 cells, as it acts as a demetallation and decarbonylation agent that mediates the conversion of thiols to disulfides. Pure culture of *E. coli* O157:H7 was decimally diluted in YPLT medium from 8.0×10^0 to 8.0×10^8 CFU mL^{-1}. Diluted cultures were incubated in a continuous rotation incubator (VWR International, West Chester, PA) and the samples were taken out for impedance measurement at an interval of 2 h from each enriched sample. Samples were immersed in a boiling water bath for 20 min to kill bacterial cells and then were stored at 4 °C until impedance measurement was performed. For the samples with initial concentrations of 8×10^6 and 8×10^8 CFU mL^{-1} of *E. coli* O157:H7, additional samples were taken out at an interval of 30 min from the start till 2 h of enrichment growth to measure the impedance response of the system over a short period of bacterial growth.

2.3. Design of double IAM-based impedance biosensor

IAM chips were obtained from ABtech Scientific Inc. (Richmond, VA), which contained a gold layer (1000 Å) sputtered on borosilicate glass substrate with an adhesion promotion layer of 100 Å titanium–tungsten alloy residing between the glass and gold layer. A topcoat layer of silicon nitride was used to passivate the busses and provide a window through which the active area of electrodes was exposed. The total size of an IAM chip was 2 cm × 1 cm × 0.05 cm with 50 pairs of fingers each of 15 μm width and 4.96 mm length. The space between the fingers was 15 μm. Before assembly, IAM chips were cleaned with 0.1 M sodium hydroxide, 0.1 M hydrochloric acid, acetone, and deionized water, and then dried in a stream of nitrogen. Two IAM chips facing each other were put together with a silicon rubber gasket (thickness 250 μm) between them to assemble a flow cell as shown in Fig. 1a. The gasket was cut in the center (5 mm × 5 mm), to expose the electrode surfaces to detection medium. Both IAM chips were tied together using an elastic band. Holes (diameter 1 mm) were drilled in each of the IAM chips to make inlet and outlet for the fluid flow. Nanoport connectors (Upchurch Scientific, Oak Harbor, WA) were bonded to the inlet and outlet in order to connect tubing for fluid flow. The assembly of the flow cell is shown in Fig. 1b.

2.4. Impedance measurement

Impedance measurement was performed using an IM-6 impedance analyzer (BAS, West Lafayette, IN) with IM-6/THALES software. For all impedance measurements, a sine-modulated ac potential of 100 mV was applied across the flow cell and a Bode plot for the magnitude of impedance and phase angle was plotted for a range of frequency from 10 Hz to 1 MHz. Samples were injected into the flow cell with the help of a syringe pump at a flow rate of 33 μL/min. To observe the effect of the presence of bacterial cells on the impedance measurement, a sample with 5.4×10^4 CFU mL^{-1} of *E. coli* O157:H7 cells after 16 h of growth was centrifuged at 250 × *g* for 15 min (supernatant was separated for impedance measurement) and was compared with a similar sample without centrifugation. The effect of live and dead bacterial cells on impedance measurement was also tested. Bacterial cells were inactivated by immersing in a boiling water bath for 30 min.

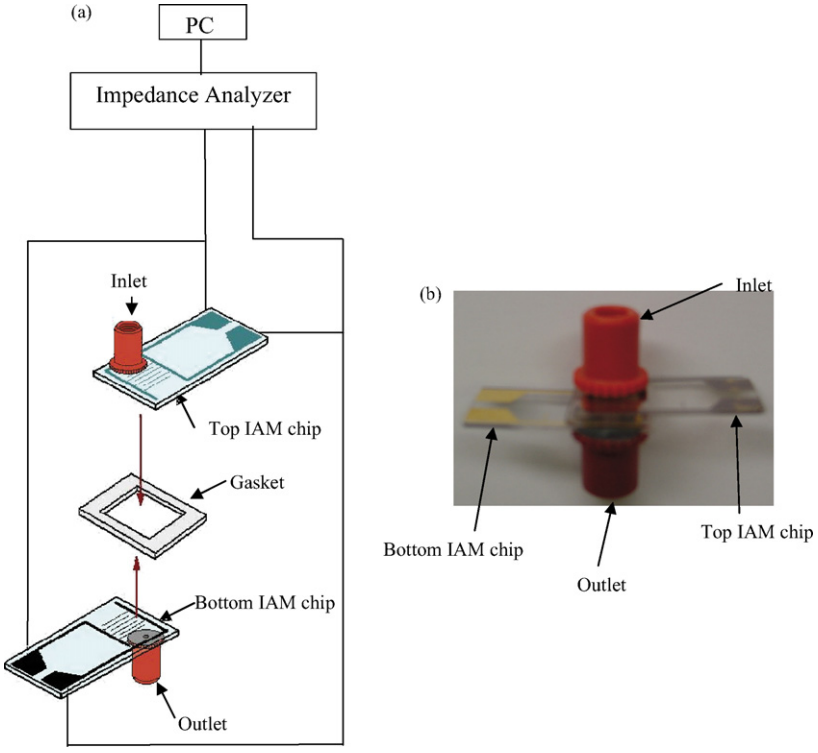

Fig. 1. (a) Schematic diagram of the assembly of double interdigitated array microelectrode-based flow cell and (b) an assembled flow cell.

To monitor the effect of frequency on impedance measurement, the normalized impedance change (NIC) was plotted against growth time for five different frequencies (10 Hz, 270 Hz, 4.18 kHz, 64.6 kHz, and 1 MHz). To plot the growth curves, NIC was plotted against growth time for different concentrations of *E. coli* O157:H7 ranging from 8.0×10^0 to 8.2×10^8 CFU mL^{-1}. NIC was calculated as follows

$$\text{NIC} = \frac{Z_{\text{sample}} - Z_{\text{control}}}{Z_{\text{control}}} \times 100 \quad (1)$$

where Z_{control} is the magnitude of impedance for control sample before growth and Z_{sample} is the magnitude of impedance for a sample containing *E. coli* O157:H7 after an enrichment growth.

3. Results and discussion

3.1. Double IAM-based versus single IAM-based flow cells

Fig. 2a shows the comparison of impedance responses of double and single IAM-based flow cells for the impedance measurement of 8.2×10^4 CFU mL^{-1} of *E. coli* O157:H7 after an enrichment growth of 16 h. The magnitude of impedance measured with double IAM decreased in the range of 61–37% for the range of frequencies from 10 Hz to 1 MHz as compared to single IAM. Since resistance is inversely proportional to the surface area, the resistive impedance for double IAM was lower than single IAM due to the availability of more surface area for impedance measurement. The microelectrodes scan a region called "active region", which has a maximum strength of an electric field and a few microns above the surface. IAM usually results in a sensitive impedance change, if bacterial cells are present in the active region [33]. Radke and Alocilja [20] calculated the range of active region for an electrode with width and space measuring 3 and 4 μm, respectively. IAM is best to detect impedance change when bacterial cells are present in the active region which is 10 μm above the surface of electrodes. When cells are present outside the active region, impedance change is minimized. The presence of IAM on both inside walls (top and bottom) of the detection chamber increases the amount of ions detected due to presence of two active regions of IAM as compared to one active region with single IAM configuration as shown in Fig. 2b. Thus, double IAM-based flow cell was more effective in improving the sensitivity of impedance measurement as compared to single IAM-based flow cell.

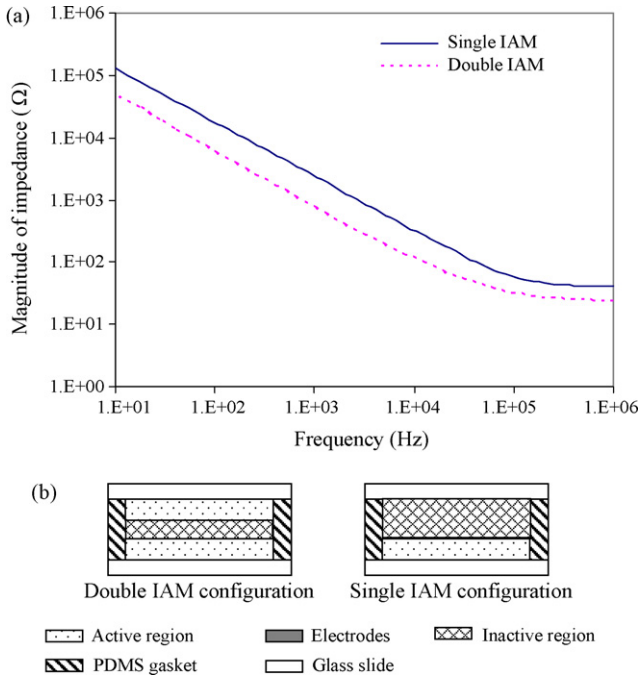

Fig. 2. (a) The magnitude of impedance measured for 8.2×10^4 CFU mL^{-1} of *Escherichia coli* O157:H7 after an enrichment growth of 16 h using double and single interdigitated array microelectrode-based flow cells and (b) schematic diagram of cross section of flow cells with double and single IAM. Double interdigitated array microelectrodes detected more ions in the detection chamber as compared to single interdigitated array microelectrode within the same detection chamber.

3.2. Equivalent circuit analysis for impedance measurement system

The experimental data of impedance biosensor in aqueous solution was represented by an equivalent circuit as shown in Fig. 3a. The equivalent circuit consisted of two double layer capacitor (C_{dl}) (one for each set of electrodes) connected in series with bulk medium resistor (R_{s}). Constant phase element was used to model double layer capacitance of the electrodes. This is commonly favored over the use of a simple capacitor [34]. C_{dl} accounted for the effect of ionic species on the capacitance near the surface of an electrode. R_{s} represented bulk resistance of the solution, accounting for the change in conductivity and charge transport across the bulk solution.

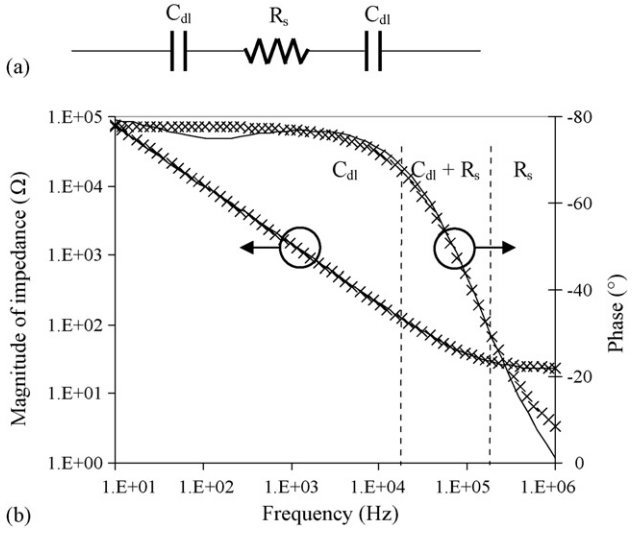

Fig. 3. (a) Equivalent circuit for the impedance measurement of growth of *E. coli* O157:H7 cells in YPLT medium using a double interdigitated array microelectrode-based flow cell and (b) experimental and curve-fitted Bode plots for the impedance measurement of 5.4×10^4 CFU mL^{-1} of *E. coli* O157:H7 after the growth of 16 h. Solid lines show the experimental data, while cross marks show curve-fitted data.

Fig. 3b shows the experimental and simulated data for impedance measurement (both magnitude and phase) of 5.6×10^4 CFU mL^{-1} of *E. coli* O157:H7 after an enrichment growth of 16 h in YPLT medium using double IAM-based flow cell. To validate equivalent circuit, 50 points of the measured data on the impedance spectrum were automatically selected by the IM-6/THALES software and were used as an input to the equivalent circuit, generating a fitting impedance spectrum. Fitting was done by the IM-6/THALES software, using a complex non-linear least-square method. The close agreement between the measured data and fitted spectra indicated that the proposed equivalent circuit provided a feasible, if not unique, model to represent the impedance measurement system. There are three regions in the impedance spectrum. These are represented by two components in the equivalent circuit individually, and their combination. The double layer region dominated by C_{dl} was in the frequency range of 10 Hz to 20 kHz. Resistive region dominated by R_s was in the frequency range of 202 kHz to 1 MHz. The region dominated by both C_{dl} and R_s was in the frequency range of 20–202 kHz.

The frequency dependent characteristics of the three regions can be explained using mathematical relationships between resistance, capacitance, frequency, and impedance. In an electric circuit, the mathematical relationships of resistance, capacitance, and their contribution to the total impedance value are given by

$$\text{resistive impedance}: \quad Z_R = R_s \tag{2}$$

$$\text{capacitive impedance}: \quad Z_c = \frac{1}{2\pi f C_{dl}} \tag{3}$$

Magnitude of total impedance due to a resistor and a capacitor:

$$|Z| = \sqrt{R_s^2 + \frac{1}{(\pi f C_{dl})^2}} \quad \text{(serial connection of } C_{dl} \text{ and } R_s\text{)} \tag{4}$$

The calculations of total impedance based on above equations clearly showed that the values of total impedance at a frequency less than 20 kHz were dominated (≥90%) by double layer capacitance (Eqs. (3) and (4)); while in between 202 kHz and 1 MHz the values of total impedance were dominated (≥90%) by bulk medium resistance (Eqs. (2) and (4)). Contributions of double layer capacitance and bulk medium resistance can also be interpreted by looking at the phase angle values shown in the impedance spectrum (Fig. 2b). The effect of the double layer capacitance at a frequency less than 20 kHz was evident by the phase angle values close to −90° as shown in the Bode plot. In this frequency range, the magnitude of impedance decreased with increase in frequency, as capacitive impedance is inversely proportional to the frequency of the applied potential (Eq. (3)). In the high frequency range from 202 kHz to 1 MHz, resistive region was evident by the phase angle values close to 0° and the magnitude of the impedance was constant for this frequency range, as resistive impedance is independent of frequency (Eq. (2)). For the frequency range of 20–202 kHz, the impedance was controlled both by capacitance and resistance, as the phase angle was in between 0° and −90°.

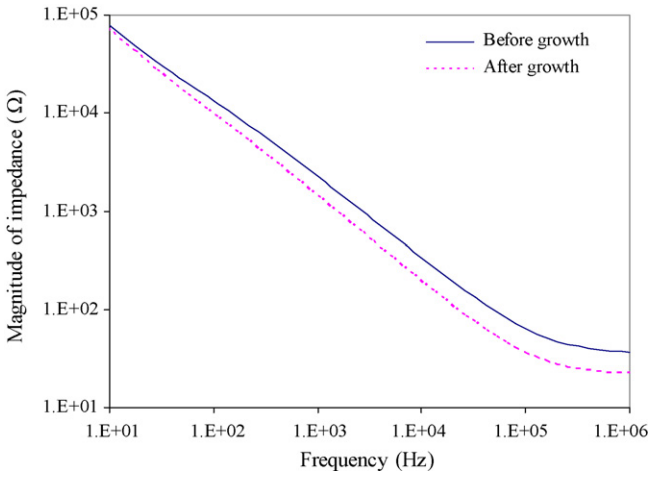

Fig. 4. Bode plot for the magnitude of impedance measured before and after an enrichment growth of 5.4×10^4 CFU mL^{-1} of *E. coli* O157:H7 cells for 16 h in YPLT medium. The impedance was measured for the range of frequencies from 10 Hz to 1 MHz.

3.3. Effect of the growth of E. coli O157:H7 cells on impedance measurement

Fig. 4 shows the impedance measurement of 5.6×10^4 CFU mL^{-1} of *E. coli* O157:H7 before and after an enrichment growth of 16 h in YPLT medium. After growth, the magnitude of impedance decreased for the entire range of frequency, especially for frequency greater than 100 kHz. In order to understand this change in the impedance, the experimental data before and after growth were curve fitted using an equivalent circuit shown in Fig. 3a. Table 1 shows the simulated values of R_s and C_{dl} for the impedance spectrum before and after the growth of *E. coli* O157:H7. Due to *E. coli* O157:H7 growth, the values of double layer capacitance increased and the bulk medium resistance decreased. Thus, change in the impedance values due to bacterial growth was due to double layer capacitance and bulk resistance of the medium, implying that the growth of *E. coli* O15:H7 cells in growth medium can be monitored by measuring the change in the double layer capacitance or the change in the bulk medium resistance in the range of frequencies from 10 Hz to 20 kHz and 202 kHz to 1 MHz, respectively.

Table 1
Simulated values of R_s and C_{dl} in the equivalent circuit for 5.4×10^4 CFU mL^{-1} of *E. coli* O157:H7 cells before and after an enrichment growth of 16 h and their respective percentage change[a] with respect to the samples before growth

	R_s (Ω)	C_{dl} (nF)
Before growth	33.96 ± 3.1	155.0 ± 11.2
After growth	22.59 ± 1.8	227.2 ± 10.1
Change (%)[a]	−33.4	+46.5

[a] Negative change indicates a decrease in parameter value and positive change indicates an increase in parameter value.

The double layer capacitance depends on many factors including electrode potential, temperature, ionic concentrations, type of ions, and electrode surface properties. The values of electrode potential and temperature were constant and hence their effect can be ignored. The value of the double layer capacitance can be expressed as [16]:

$$C_{dl} = \frac{\varepsilon_{dl} A}{d} \quad (5)$$

where ε_{dl} is the dielectric permittivity of the double layer, $\varepsilon_{dl} = \varepsilon_0 \varepsilon_r$, ε_0 the permittivity of the free space and ε_r the relative permittivity of the layer separating ionic charges and the electrode, A the area of the electrode, and d is the thickness of double layer. Substrates present in the microbiological growth medium are generally uncharged or weakly charged but are transformed into highly charged end products as microorganisms to follow metabolic pathways. This results in an increase in the conductivity of the test medium and a decrease in impedance [5]. Metabolic activities during bacterial growth of *E. coli* O157:H7 cells converted uncharged or weakly charged substrates (lactose, yeast extract, peptone, and TMAO) present in YPLT medium into highly charged ions. For example, TMAO was reduced into trimethylamine cations and lactose was metabolized into acid. All these highly charged ions formed in the medium caused an increase in the permittivity of the medium and a decrease in the thickness of the double layer at the same time. These changes together resulted in an increase in the values of C_{dl} and consequently a decrease in the impedance. The decrease in the bulk medium resistance after growth of bacterial cells was also caused by an increase in the concentration of highly charged ions in the medium.

Previous researches related to IAM-based impedance detection systems have shown that during impedance measurement, cells attached to the electrodes do not contribute directly to the double layer capacitance [16,35]. Our results clearly showed that the presence of bacterial cells in the detection sample did not affect the impedance response of the sensor (data not shown). Impedance response of the sensor for bacterial cells was measured for the sample with initial concentration of 5.4×10^4 CFU mL^{-1} of *E. coli* O157:H7 after 16 h of growth. This was compared with the impedance response of the sensor after centrifuging the same sample to remove bacterial cells (supernatant was used for impedance measurement). Previous research had reported that the cell membrane (thickness 5–10 nm) has a capacitance of 0.5–2.5 μF/cm^2 and a resistance of 10^2 to 10^5 Ω cm^2 [34]. The double layer capacitance will only be affected by the presence of cells, if they lie within its thickness, which is typically of the order of several angstroms [36]. Cells attached either specifically or non-specifically to electrodes do not lie within this thickness, hence, they do not directly affect double layer capacitance [37]. In addition to this, the aqueous gap between cells and the electrode surface prevents direct effect of the cell membrane on the interfacial impedance of the electrodes [38]. Therefore, in our research the increase in double layer capacitance was not due to bacterial attachment, but was caused by the change in ionic composition of the double layer. Thus, this change can directly be related to the presence of highly charged by-products produced during bacterial metabolism.

3.4. Effect of frequency on impedance measurement

To monitor the effect of frequency on impedance measurement, the values of NIC were calculated at different frequencies (Eq. (1)), and plotted against growth time. Fig. 5 shows the NIC *versus* growth time for the impedance measurement of the sample with initial concentration of 5.4×10^4 CFU mL^{-1} of *E. coli* O157:H7 at five different frequencies. The values of NIC for all five frequencies decreased with an increase in growth time. The decrease in the values of NIC was more at higher frequencies. Maximum change in the values of NIC with respect to the growth time was observed in the initial 6–8 h growth of bacterial cells. Between 8 and 16 h of growth, the change in the values of NIC was not significantly different ($P > 0.05$). After 6–8 h of growth, maximum changes in the values of NIC were 7.8%, 10.9%, 17.6%, 25.5%, and 30.5% for impedance measurements at frequencies of 10 Hz, 270 Hz, 4.18 kHz, 64.6 kHz, and 1 MHz, respectively. Based on this observation, 1 MHz was chosen to monitor the change in the impedance values corresponding to the growth of *E. coli* O157:H7 cells using double IAM-based flow cell. Bacterial cells were in the "log phase" of growth after a short "lag phase", during which they grow exponentially and produce a huge amount of by-products and thus maximum decrease in the values of NIC was observed during initial 6–8 h of growth of bacterial cells. The food and nutrients available for the bacteria get exhausted as bacterial growth progresses and thus, bacteria tend to shift to "stationary phase" of growth, where the production of by-products is limited and hence, no significant change in the values of NIC was observed between 8 and 16 h of growth of bacterial cells.

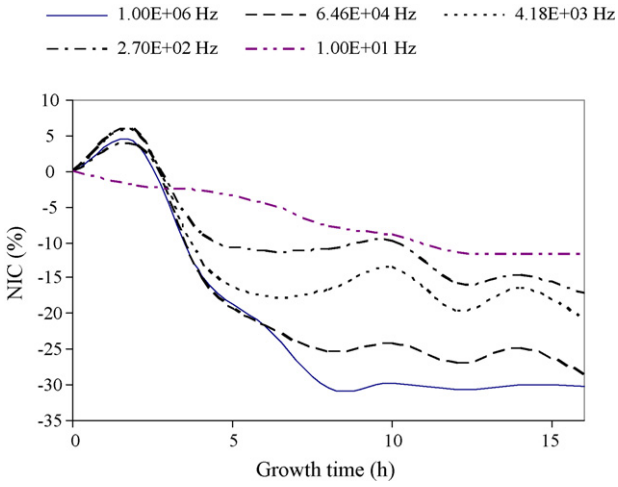

Fig. 5. Normalized impedance change (NIC) *vs*. growth time for the impedance measurement of 5.4×10^4 CFU mL^{-1} of *E. coli* O157:H7 at frequencies of 10 Hz, 270 Hz, 4.18 kHz, 64.6 kHz, and 1 MHz.

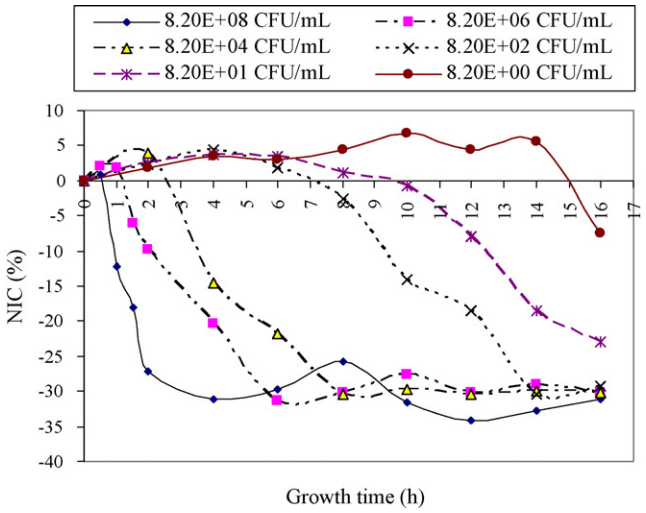

Fig. 6. Growth curves (NIC *vs.* growth time) for a range of 8.0×10^0 to 8.2×10^8 CFU mL^{-1} of *E. coli* O157:H7 cells after an enrichment growth in YPLT medium.

3.5. Detection of E. coli O157:H7 inside the double IAM-based flow cell

The values of NIC calculated at 1 MHz were used to quantify the initial numbers of bacterial cells present in the original samples after an enrichment growth in YPLT medium. Fig. 6 shows the growth curves (NIC *versus* growth time) for a range of initial concentrations of *E. coli* O157:H7 cells from 8.0×10^8 to 8.2×10^8 CFU mL^{-1} present in the sample. The values of NIC were positive at the beginning and then started to decrease. The time when impedance values start to decrease as compared to the NIC values at $t = 0$ h is taken as the detection time. The detection time decreased with increase in the initial numbers of *E. coli* O157:H7 cells present in the sample before growth. High number of cells in the sample at time $t = 0$ h resulted in a rapid change in the conductivity of the solution due to fast bacterial metabolism. As a result of this, high initial number of *E. coli* O157:H7 present in the samples were detected in low detection time and vice versa. Fig. 7 shows the detection time for different concentrations of *E. coli* O157:H7 ranging from 8.0

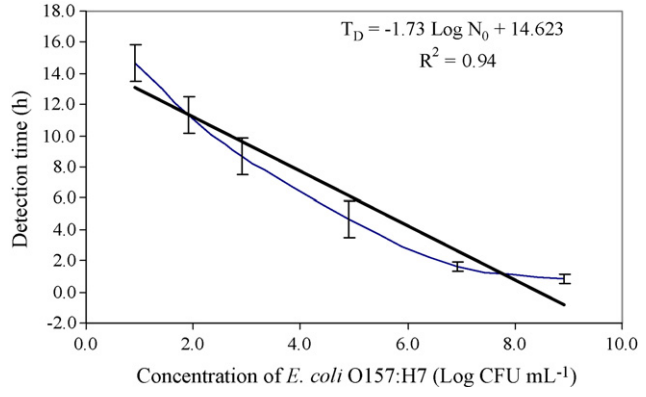

Fig. 7. The linear relationship between the logarithmic values of *E. coli* O157:H7 concentrations and detection times obtained from the impedance measurement of samples at different sampling times after the growth of bacterial cells.

to 8.2×10^8 CFU mL^{-1}. The detection times for 8.0, 8.2×10^1, 8.2×10^2, 8.2×10^4, 8.2×10^6, and 8.2×10^8 CFU mL^{-1} were 14.7, 11.3, 8.7, 4.7, 1.7, and 0.8 h, respectively. The detection time was calculated based on the average of three readings. In this study, an indirect impedance detection method has been used for quantifying initial number of *E. coli* O157:H7 cells present in the sample.

Some researchers have reported that the direct detection of *E. coli* O157:H7 cells in the samples. Suehiro et al. [27] used dielectrophoresis to align 10^5 CFU mL^{-1} of *E. coli* O157:H7 in between the electrodes and the impedance, measurement was conducted in the presence of a low conductivity medium (0.1 M mannitol solution and conductivity 0.2 mS/m) without any enrichment growth. The "pearl bead" formation of cells in between the electrodes acted as conductor. *E. coli* O157:H7 cells behaved as conductor in the presence of mannitol solution as some components of bacterial cells (i.e., cell wall and cytoplasm) were more conductive than the mannitol solution (conductivities of cell wall and cytoplasm are 500 mS/m and 100 mS/m, respectively) [29]. In other studies, the *E. coli* O157:H7 cells were attached to antibodies present on the surface of electrodes and impedance measurement was performed in the presence of a highly conductive redox probes [20,23].

4. Conclusions

Double IAM-based flow cell was successfully used in an impedance biosensor for the detection of *E. coli* O157:H7 in a range from 8.0 to 8.2×10^8 CFU mL^{-1} after an enrichment growth of 14.7 and 0.8 h, respectively. Double IAM-based flow cell was effective in improving the sensitivity of impedance detection by providing more surface area as compared to the single IAM-based flow cell. The equivalent circuit analysis indicated that the change in impedance values due to bacterial growth was caused by both double layer capacitance and bulk medium resistance, and these parameters in turn were the function of the amount of charged ions present in the medium. Specificity of this impedance biosensor could be ensured by the use of selective growth medium or immunoseparation based on magnetic microbeads conjugated with antibodies specific to target bacteria. Impedance measurement in a flow cell can be useful to design a portable instrument for monitoring bacterial cell growth and their metabolites.

Acknowledgments

This project was supported in part by USDA/FAS and the Food Safety Consortium.

References

[1] O.N. Okigbo, G.H. Richardson, J. Food Prot. 48 (1985) 978.
[2] J. Strassburger, J. Hossbach, R. Seidel, Int. J. Med. Microbiol. 274 (1991) 481.
[3] G. Kroyer, K. Futschik, A. Gschwandtner, Proceedings of the 8th European Conference on Food Chemistry, Austrian Chemical Society, Vienna, Austria, September 18–20, 1995, pp. 555–561.
[4] P. Silley, S. Forsythe, J. Appl. Bacteriol. 80 (1996) 233.

[5] M. Wawerla, A. Stolle, B. Schalch, H. Eisgruber, J. Food Prot. 62 (1999) 1488.
[6] R. Gomez-Sjöberg, T. Morisette, R. Bashir, J. Microelectromech. Syst. 14 (2005) 829.
[7] G.N. Stewart, J. Exp. Med. 4 (1899) 235.
[8] A. Edmiston, A. Russell, J. Food Prot. 61 (1998) 1375.
[9] C.J. Felice, M.E. Valentinuzzi, IEEE Trans. Biomed. Eng. 46 (1999) 1483.
[10] B.C. Towe, V.B. Pizziconi, Biosens. Bioeletron. 12 (1997) 893.
[11] C. Berggren, B. Bjarnason, G. Johansson, Biosens. Bioelectron. 13 (1998) 1061.
[12] V.M. Mirsky, M. Mass, C. Krause, O.S. Wolfbeis, Anal. Chem. 7 (1998) 3674.
[13] J. Min, A. Baeumner, Electroanalysis 16 (2004) 724.
[14] C. Amatore, B. Fosset, J. Bartelt, M.R. Deakin, R.M. Wighman, J. Electroanal. Chem. 256 (1988) 255.
[15] M. Ciszkowska, Z. Stojek, J. Electroanal. Chem. 466 (1999) 129.
[16] L. Yang, Y. Li, C.L. Griffis, M.G. Johnson, Biosens. Bioelectron. 19 (2004) 1139.
[17] L. Yang, Y. Li, J. Microbiol. Methods 64 (2006) 9.
[18] R. Gomez, R. Bashir, A. Sarikaya, M.R. Ladisch, J. Sturgis, J.P. Robinson, T. Geng, A.K. Bhunia, H.A. Apple, S. Wereley, Biomed. Microdev. 3 (2001) 201.
[19] R. Gomez, R. Bashir, A.K. Bhunia, Sens. Actuator B 86 (2002) 198.
[20] S.M. Radke, E.C. Alocilja, IEEE Sens. J. 4 (2004) 434.
[21] S.M. Radke, E.C. Alocilja, Biosens. Bioelectron. 20 (2005) 1662.
[22] S.M. Radke, E.C. Alocilja, IEEE Sens. J. 5 (2005) 744.
[23] L. Yang, Y. Li, G.F. Erf, Anal. Chem. 76 (2004) 1107.
[24] L. Yang, Y. Li, Biosens. Bioelectron. 20 (2005) 1407.
[25] F. Aldaeus, Y. Lin, J. Roeraade, G. Amberg, Electrophoresis 26 (2005) 4252.
[26] H. Li, R. Bashir, Sens. Actuator B 86 (2002) 215.
[27] J. Suehiro, R. Yatsunami, R. Hamada, M. Hara, J. Appl. Phys. 32 (1999) 2814.
[28] J. Suehiro, D. Noutomi, R. Hamada, M. Hara, IEEE (2001) 1950.
[29] J. Suehiro, R. Hamda, D. Noutomi, M. Shutou, M. Hara, J. Electrostat. 57 (2003) 157.
[30] B. Chang, C. Chen, S. Ding, D.C. Chen, H. Chang, Sens. Actuator B 105 (2005) 159.
[31] R. Zhou, P. Wang, H. Chang, Electrophoresis 27 (2006) 1376.
[32] S.K. Kim, P.J. Hesketh, C. Li, J.H. Thomas, H.B. Halshall, W.R. Heineman, Biosens. Bioeletron. 20 (2004) 887.
[33] P.V. Gerwen, W. Laureyn, W. Laureys, G. Huyberechts, M. Beeks, K. Baert, J. Suls, W. Sansen, P. Jacobs, L. Hermans, R. Mertens, Sens. Actuator B 49 (1998) 73–80.
[34] S. Gawad, K. Xheung, U. Seger, A. Bertsch, P. Renaud, Lab Chip 4 (2004) 241.
[35] J. Weigener, C.R. Keese, I. Giaever, Exp. Cell Res. 259 (2000) 158.
[36] A.J. Bard, L.R. Faulkner, Electrochemical Methods: Fundamentals and Applications, 2nd ed., John Wiley and Sons, New York, 2000, pp. 368–416.
[37] D. Gingell, Cell contact with solid surfaces, in: R. Galser, D. Gingell (Eds.), Biophysics of the Cell Surface, Springer, New York, 1990, pp. 263–268.
[38] I. Giaever, C.R. Keese, Proc. Natl. Acad. Sci. 88 (1991) 7896.